# Using hydraulic equivalences to discriminate transport processes of volcanic flows.

Alain Burgisser, James E. Gardner

# Using hydraulic equivalences to discriminate transport processes of volcanic flows[1]

**Alain Burgisser**

*Institut des Sciences de la Terre d'Orléans, CNRS - Université d'Orléans, 45071 Orléans, France*

**James E. Gardner**

*Department of Geological Sciences, University of Texas at Austin Austin, Texas 78712-0254, USA*

## ABSTRACT

We characterized stratified deposits from Upper Toluca Pumice at Toluca Volcano, Mexico, to distinguish the various modes of transport at play in their genesis. Using the concept of hydraulic equivalence, we determined that deposits resulted from a combination of suspended-load fallout, saltation, and rolling. In particular, some well-sorted coarse stratified beds have a single pumice mode most likely indicative of clasts having traveled through both the transport system and the traction bed. Such beds are likely remnants of the sorting operated within the large-scale transport system. Other coarse beds have pumice and lithic modes suggesting rolling in the traction bed. We propose that boundary layer processes control the sorting of those beds and all finer beds. By helping to discriminate between transport mechanisms, hydraulic equivalences have a general applicability in geophysical flows involving clasts of contrasted densities.

**Keywords:** hydraulic equivalence, stratified deposit, sedimentation, volcanic eruption, surge.

[1] GSA Data Repository item 2005##, stratigraphic logs, field photographs, and sedimentological analysis, is available online at www.geosocitey.org/pubs/ft2005.htm, or on request from editing@geosociety.org or Documents Secretary, GSA, PO Box 9140, Boulder, CO 80301-9140, USA.

## INTRODUCTION

Nearly all volcanoes feature stratified pyroclastic deposits composed of well to moderately sorted cross- and planar beds (e.g., Cas and Wright, 1987). Despite the ubiquity of such deposits, we only have a crude understanding of their genesis. Moreover, stratified deposits often record superimposed origins, because fall and pyroclastic density currents are only end-members of a continuum of volcanic flows (Wilson and Hildreth, 1998). Distinguishing between the various modes of transport at play is a necessary step toward accessing crucial information about the parent flow and the associated eruptive regime.

In an attempt to discriminate transport processes, we review and develop the concept of hydraulic equivalence, which states under what conditions clasts of various sizes and densities are similarly transported. This method is then applied to grain-size data from stratified deposits that are part of the Upper Toluca Pumice (UTP) at Nevado de Toluca Volcano, Mexico (Fig. 1).

## HYDRAULIC EQUIVALENCES

Models of volcanic flows invoke several processes of sedimentation that generate stratified deposits, including suspended-load fallout, saltation, rolling and gravity grain flow (Wohletz and Sheridan, 1979; Fisher, 1990; Valentine, 1987; Sohn, 1997). We disregard gravity grain flow as a process occurring in most pyroclastic stratified deposits because cross-beds almost always dip less steeply than the angle of repose. We propose to discriminate between the remaining three mechanisms through their potential for sorting particles by size and density. In each case, hydraulic equivalence is reached when particles (pumice and lithics) have a similar (usually steady-state) motion.

Suspended-load fallout occurs when particles that are carried mainly by large-scale turbulent motions of hot gases sediment from the pyroclastic cloud (Valentine, 1987). Clasts fall at their terminal fall velocity ($U_T$), which is given by (Crowe et al., 1997):

$$U_T = \frac{4\rho d^2 g}{3\mu C_D Re} \quad \text{(1a)}$$

$$C_D = \frac{24}{Re} + \frac{3.6}{Re^{0.313}} + \frac{0.42}{Re + 42500 Re^{-0.16}}, \; Re{<}10^5 \qquad \text{(1b)}$$

where $\rho$ is clast density, $d$ is clast diameter, $\mu$ is (dusty) gas viscosity, $Re$ is particle Reynolds number ($=U_T\, d/\upsilon$), $\upsilon$ is kinematic viscosity of the (dusty) gas, $g$ is gravity acceleration, and $C_D$ is a drag coefficient. Hydraulic equivalence for fallout (including from suspension) is reached when pumice of density $\rho_1$ and size $d_1$ have the same terminal velocity as lithics of density $\rho_2$ and size $d_2$ (Fig. 5b). We use hot air ($\mu$=1.5 $10^{-5}$ Pa s, $\upsilon$=3 $10^{-5}$ m$^2$/s) in this study, noting equivalences are little affected by values of $\mu$ and $\upsilon$. Analytical solutions of (1) can be found using $C_D = 24/Re$ for Stokes flow and $C_D$~0.45 at large $Re$:

$$\rho_1 d_1^{\,2} \cong \rho_2 d_2^{\,2} \; \text{for } Re{<}10 \quad \text{(2a)}$$

$$\rho_1 d_1 \cong \rho_2 d_2 \; \text{for } Re{>}10^3 \quad \text{(2b)}$$

At low $Re$, lithics fall at the same speed as pumice that are $\sim\sqrt{\rho_2/\rho_1}$ larger, whereas at high $Re$, lithics fall at the same speed as pumices that are $\rho_2/\rho_1$ larger. Hence, suspended-load fallout sorts clasts as a function of both size and density, with more marked sorting for larger clasts.

Clasts may saltate steadily if the current supplies enough energy to balance that lost during bouncing. Considering that clasts usually reach their terminal fall velocity before impact (Hanes and Bowen, 1985), the airborne part of the motion sorts between clasts according to (1)-(2). To what extent, however, repeated bouncing, which is confined to a short part of the motion, affects sorting? Typically, bouncing clasts keep between 20 and 60% of their kinetic energy, 10–40% of which is rotational. The total kinetic energy of a steadily saltating clast before impact is thus (Chau et al., 2002):

$$E_k = A\frac{\pi}{12}d^3\rho U_T^2 \quad (3)$$

where $A$ is a coefficient between 1.1 and 1.4 taking account of rotation. Hydraulic equivalence for the conserved part of the kinetic energy occurs when, at equivalent velocity before impact, clasts lose the same amount of energy during rebound:

$$\rho_1 d_1^{\,3} = \rho_2 d_2^{\,3} \quad (4)$$

The scatter of experimental data (Chau et al., 2002; Cagnoli and Manga, 2003) suggests rebound angle, clast shape, and the nature of the surface may exert a greater control on the amount of energy dissipated during rebound than the difference in material properties between pumice and lithics (i.e., strength and density). One can nevertheless expect that pumices deform and/or break more easily than lithics, which compensates somewhat the equivalence in (4) by allowing lithics to conserve a higher kinetic energy than pumice, all other parameters being equal. Thus, despite pumices slowing down more markedly than lithics during rebound, the airborne trajectory tend to dominate the way saltation segregates clasts.

Clasts rolling down freely a rough surface made of identical particles can reach constant velocity depending on the inclination of the surface. The total kinetic energy of a rolling clast is (Dippel et al., 1996):

$$E_k = \frac{7\pi}{60}\rho\, d^3 v_t^2 \quad (5)$$

where $v_t$ is tangential velocity. As a clast rolls from one bed particle to the next, it loses speed because of the sharp change in direction. By energy balance, tangential speeds before ($v_i$) and after ($v_f$) the collision are related by (Dippel et al., 1996):

$$v_f = v_i \sqrt{1 - \frac{20}{7} \frac{\lambda^2 d(d+2\lambda)}{(d+\lambda)^4}} \quad (6)$$

where λ is diameter of bed particles. To maintain steady-state rolling on a horizontal surface, we propose that the loss in kinetic energy from one bed particle to the next must be balanced by the work done by a external force $F_t$ over the length of a bed particle diameter:

$$\lambda F_t = \frac{\pi}{3} \rho d^4 \lambda^2 v_i^2 \frac{(d+2\lambda)}{(d+\lambda)^4} \quad (7)$$

We consider for now that $F_t$ is some average force ($F_t \sim \rho^m d^n$) that the current steadily applies on the rolling clasts. Using (5)-(7), hydraulic equivalence for steady-state rolling becomes:

$$\rho_1^{(1-m)} d_1^{(4-n)} \frac{(d_1+2\lambda)}{(d_1+\lambda)^4} = \rho_2^{(1-m)} d_2^{(4-n)} \frac{(d_2+\lambda)}{(d_2+\lambda)^4} \quad (8)$$

If $F_t$ is related to the shear applied by the air/dusty gas, it likely depends on both size and density ($m \rightarrow 1$, $n>0$), and hydraulic equivalence is only ensured for clasts of identical sizes. On the other hand, if $F_t$ is mostly due to closely-spaced impacts from other moving particles, like under packed conditions, it may be independent of size and density ($m,n=0$). The equivalence ($d_1/d_2$) varies then from $(\rho_2/\rho_1)^{0.4}$ to $\rho_2/\rho_1$ as the substratum change from rough ($\lambda=d_1$) to smooth ($\lambda=d_1/1000$), respectively, and sorting is similar to that of airborne transport. If rolling is triggered by an impulsive force, such as infrequent collisions, $F_t$ cannot be averaged. Instead, clasts are suddenly accelerated and roll freely on the rough surface until the next impulse. Rolling is then a sole function (Dippel et al., 1996) of the initial angular velocity ($v_\phi$), which is related to the impulsive tangential force ($F_i$) applied to the clast surface by (Schmeeckle and Nelson, 2003):

$$F_i = \frac{\pi}{15} \rho d^4 \frac{dv_\phi}{dt} \quad (9)$$

Hydraulic equivalence of impulsive rolling is reached when a given impulse leads to a similar angular acceleration for both particles:

$$\rho_1 d_1^4 = \rho_2 d_2^4 \quad (10)$$

Thus, lithics would roll along with pumices that are $\sqrt[4]{\rho_2/\rho_1}$ larger. Hence, rolling sorts clasts mostly by size and only weakly by density compared to fallout and saltation, except when caused by a force independent of clast size and density.

Our analysis shows saltation, fallout, and packed rolling cannot be discriminated solely on the basis of sorting and will thus be considered together. Shear- and collision-induced rolling, however, can be discriminated from the other mechanisms if pumice densities differ greatly from lithic densities and have a restricted range. This is the case at Toluca, where a Kolmogorov-Smirnov test with densities measured at UTP shows that sorting differences are statistically significant even for small grain sizes.

**STRATIFIED DEPOSITS OF THE UTP**

The most recent Plinian eruption of Toluca volcano produced the 10445 ± 95 B.P. dacitic UTP (Arce et al., 2003), which consists of four successive Plinian fall units ($PC_0$-$PC_3$) interlayered with three pyroclastic density current units ($F_0$-$F_2$). Our focus is on the better-preserved pyroclastic unit, $F_1$, which is composed of a Basal unit that has mainly stratified layers, a well sorted Middle unit, and a Top unit (Fig. 1). The Middle unit has characteristics typical of fall deposits mixed with some products of pyroclastic current (relevant data supporting this interpretation are in the electronic supplement). Overall, thinner parts of the Top unit tend to be on paleo-highs and feature stratified layers, whereas thicker parts fill paleovalleys and generally consist of multiple massive, poorly sorted subunits. At some locations, pumice levees and paleo-gullies indicate that the flow was channeled. These flow lines mostly follow the general slope of the topography, from the vent down to the surrounding plain. Massive units can be traced laterally into stratified layers and, in one exposed area, a massive unit merges downstream into stratified unit (Fig. 2).

We made representative samplings of the stratified deposit by collecting 9 individual beds at 4 locations and 12 bulk samples at 8 locations (Fig. 1, see electronic supplement for detailed description). Six of these 21 samples were from the Basal unit, the others being from the Top unit. We collected 6 representative samples from massive deposits in the Top unit. We also measured the downstream wavelength and amplitude of 39 dunes, and the downstream length and thickness of 14 planar beds (Fig. 3).

Stratified layers are composed of, on average, 36 wt.% angular to poorly rounded pumice, 26 wt.% angular lithics, 23 wt.% crystals, and 15 wt.% glass. They have no systematic vertical or horizontal trend in pumice-to-lithic ratio, and the stratification angle of cross-beds is always <20°. Bulk samples of stratified layers are poorly sorted and polymodal, with modes around $-3.5\ \phi$, $-1.5\ \phi$, and $2\ \phi$ (Fig. 4a). Individual beds, in contrast, are moderately to well-sorted with size distributions dominated by one of the modes of the bulk deposit (Fig. 4b). Density sorting of the modes is similar for all grain sizes, except for the coarsest modes of some samples, which are richer in pumice (Fig. 4c). This double sorting of sizes and densities can be seen in the field because well-sorted layers of coarse pumice are easily distinguished from finer layers of mixed clasts. These coarse layers are common, although less abundant than finer beds.

They contain either subordinate lithics with sizes similar to those of pumices, or very few lithics with ill-defined modes (Fig. 5a). Interestingly, coarse lithic-rich beds are absent. Coarser planar beds are thicker and more extensive than finer planar beds (Fig. 3), and they often develop downstream from an oversized clast. Dune-forms consist of stacked cross-beds that often built around a small irregularity of the substratum. Like planar beds, height and length of dunes are related by a power law (Fig. 3). There is no relationship between dune size and distance from vent.

We analyzed samples from a transitional zone where a poorly-sorted massive deposit grades downstream over a distance of 10 m into sub-horizontal beddings that are either massive or well-sorted in coarser clasts (Fig. 2a). No sorting occurs between the massive deposit and the massive beds; samples are indistinguishable (Fig. 2b-c). When comparing the massive deposit with coarse beds, we note that little density sorting occurs (Fig. 2c). Coarse beds are thus evenly depleted in finer sizes compared to the neighboring massive deposit, and have one dominant mode of pumice and lithics, respectively (ATO128, Fig. 5a).

## DISCUSSION

We used the lithic and pumice modes from a sample of the fall deposit $PC_2$ to verify the hydraulic equivalence we determined for fallout (Fig. 5). The magnitude of the error suggests grain size distributions determined at 1 $\phi$ intervals, like that of $PC_2$, poorly resolve pumice and lithic modes. Half $\phi$ intervals, like those of the other samples, are necessary to resolve hydraulic equivalences.

The presence of a mixed fall layer suggests the Top and Basal units were emplaced by two short partial collapses of an eruptive column. The absence of systematic component gradation within the stratified layers of these units precludes that inter-bed variations were caused by fluctuations of component proportion at the vent. Hence, all sedimentological variations resulted instead from transport or sedimentary processes.

Sorting in the UTP stratified deposits is best expressed in the coarser beds. Some coarse beds have similar modes of pumice and lithic (ATO7, Fig. 5a), which suggest they deposited by rolling (Fig. 5b). Other coarse beds, however, display no lithic mode (ATO110, ATO126, Fig. 5a). If those beds were the product of a single mechanism, there should be large amounts of lithics with a size depending of the specific mechanism. If, however, several processes occur simultaneously, shear- and collision-induced rolling could reinforce the sorting of clasts deposited by the other processes by remobilizing smaller grains of all densities, mixing them as a result of size-dominated sorting. In this case, coarse pumices would naturally concentrate because they are the largest clasts available.

At the transition between massive and stratified deposit, the absence of density sorting of coarse, well-sorted layers (ATO128, Fig. 5a) suggests that airborne transport played a negligible role in producing the transition. This is consistent with vanishing bed-load transport, where particle collisions become less frequent and rolling becomes a prevailing mode of transport as the depositional boundary layer evolves from dense to dilute.

Our findings are consistent with a depositional system forming a “traction carpet” (Sohn, 1997) that is composed of rolling and possibly saltating particles, upon which variable amounts of suspended load falls from the transport system. We propose that shear- and collision-induced rolling cause clasts to segregate by size and forms moving sheets of a few particle diameters thick. Assuming that the width of planar beds are on the same order as their measured length (Fig. 3), sheets are a few square decimeters, with those dimensions increasing to square meters with particle coarsening. The good sorting of most horizontal planar beds suggests those sheets did not interpenetrate, but rather came to rest by stacking, forming the stratified beds. Sheet truncation occurs if the substratum (usually previously deposited sheets) is irregular. The absence of extensive pumice rounding indicates the sheets transported clasts over short distances, most likely less than hundreds of meters. Similar bedload sheets have been observed in river sedimentation (Whiting et al., 1988).

The absence of hydraulic equivalences for some well-sorted, coarse-grained beds suggests they could be composed of clasts traveling through both the transport system and the traction bed. It is doubtful that only rolling produced such beds, because conditions are not likely to evolve from dense to dilute just before deposition, as would be implied by clasts rolling under packed conditions before being deposited by shear- or collision-induced rolling. We propose instead that such beds are the lighter remnants of the sorting operated within the large-scale transport system (i.e., suspended-load fallout), whereas boundary layer processes (i.e., traction carpet) control the sorting of other beds. Clasts coming from suspended-load fallout give crucial parameters about the transport system, such as carrying capacity, or eddy size and speed (Burgisser and Bergantz, 2002). To identify such clast populations, we suggest a strategy of sampling stratified deposits at the outcrop scale (deposit thickness and ~10 times as much horizontally) including selective sampling of the coarsest beds rich in lighter components. Although less accurate, the largest mode of bulk samples may also be used because it often corresponds to such coarse beds (Fig. 4).

Some pyroclastic deposits feature progressive distributions of wavelength of dune-forms with distance from source (Sigurdsson et al., 1987). Stratified deposits in the UTP are not progressively distributed, which might have resulted from the short distance over which these deposits occur. Each of the two pulses composing $F_1$ produced a full spectrum of stratified deposits with low bed angle, self-similar planar beds and dunes, coarse pumice-rich beds, and finer, well-sorted beds. All these characteristics are shared by many stratified deposits (Fig. 3; Cas and Wright, 1987). The fact that such a small flow can generate most of the features displayed in ignimbrites orders of magnitude more voluminous suggests the sequence of mechanisms presented herein may operate elsewhere than Toluca.

By helping to discriminate between various transport mechanisms, hydraulic equivalences have a general applicability in cases where the origin of deposit is uncertain, such as Aeolian reworking of pyroclastic material (Smith and Katzman, 1991), hybrid fall layers (Wilson and Hildreth, 1998), or coeval fall and surge (Valentine and Giannetti, 1995). Furthermore, equivalences may be extended to other transport mechanisms, such as gravity grain flow, as well as to other geophysical flows where clasts of contrasted densities are involved.

## ACKNOWLEDGMENTS

We would like to thank J.-L. Macìas for introducing us to Nevado de Toluca, and J.-L. Arce and K. Cervantes for their help in the field. AB also thanks J.-L. Bourdier for stimulating discussions. We thank G. Valentine, Y.K. Sohn, H.D. Granados, L. Capra, and an anonymous reviewer for reviews. Funding was provided by NSF grant EAR-0309703.

## REFERENCES CITED

Arce, J.L., Macia, J.L., and Vazquez-Selem, L., 2003, The 10.5 ka Plinian eruption of Nevado de Toluca volcano, Mexico: Stratigraphy and hazard implications: Geological Society of America Bulletin, v. 115, p. 230–248.

Arce, J.L., 2003, Condiciones pre-eruptivas y Evolución de la Erupción Pliniana Pómez Toluca Superior, Volcán Nevado de Toluca [PhD thesis]: Universidad Nacional Autonoma de Mexico, 136 p.

Burgisser, A., and Bergantz, G.W., 2002, Reconciling pyroclastic flow and surge: The multiphase physics of pyroclastic density currents: Earth and Planetary Science Letters, v. 202, p. 405–418.

Cagnoli, B., and Manga, M., 2003, Pumice-pumice collisions and the effect of the impact angle: Geophysical Research Letters, v. 30, p. 1636.

Cas, R.A.F., and Wright, J.V., 1987, Volcanic successions: Modern and ancient: London, Allen & Unwin, 528 p.

Chau, K.T., Wong, R.H.C., and Wu, J.J., 2002, Coefficient of restitution and rotational motions of rockfall impacts: International Journal of Rock Mechanics and Mining Sciences, v. 39, p. 69–77.

Crowe, C., Sommerfeld, M., and Tsuji, Y., 1997, Multiphase flows with droplets and particles: CRC Press, USA, 496 p.

Dippel, S., Batrouni, G.G., and Wolf, D.E., 1996, Collision-induced friction in the motion of a single particle on a bumpy inclined line: Physical Review E, v. 54, p. 6845–6856.

Fisher, R.V., 1990, Transport and deposition of a pyroclastic surge across an area of high relief: The 18 May 1980 eruption of Mount St. Helens, Washington: Geological Society of America Bulletin, v. 102, p. 1038–1054.

Hanes, D.M., and Bowen, A.J., 1985, A granular-fluid model for steady intense bed-load transport: Journal of Geophysical Research, v. 90, p. 9149–9158.

Schmeeckle, M.W., and Nelson, J.M., 2003, Direct numerical simulation of bedload transport using a local, dynamic boundary condition: Sedimentology, v. 50, p. 279–301.

Sigurdsson, H., Carey, S.N., and Fisher, R.V., 1987, The 1982 eruptions of El Chichon volcano, Mexico (3): Physical properties of pyroclastic surges: Bulletin of Volcanology, v. 49, p. 467–488.

Smith, G.A., and Katzman, D., 1991, Discrimination of eolian and pyroclastic-surge processes in the generation of cross-bedded tuffs, Jemez Mountains volcanic field, New Mexico: Geology, v. 19, p. 465–468.

Sohn, Y.K., 1997, On traction-carpet sedimentation: Journal of Sedimentary Research, v. 67, p. 502–509.

Valentine, G., 1987, Stratified flow in pyroclastic surges: Bulletin of Volcanology, v. 49, p. 616–630.

Valentine, G.A., and Giannetti, B., 1995, Single pyroclastic beds deposited by simultaneous fallout and surge processes: Roccamonfina volcano, Italy: Journal of Volcanology and Geothermal Research, v. 64, p. 129–137.

Whiting, P.J., Dietrich, W.E., Leopold, L.B., Drake, T.G., and Shreve, R.L., 1988, Bedload sheets in heterogeneous sediment: Geology, v. 16, p. 105–108.

Wilson, C.J.N., and Hildreth, W., 1998, Hybrid fall deposits in the Bishop Tuff, California: A novel pyroclastic depositional mechanism: Geology, v. 26, p. 7–10.

Wohletz, K.H., and Sheridan, M.F., 1979, A model of pyroclastic surge: Geological Society of America Special Paper, v. 180, p. 177–194.

**FIGURE CAPTIONS**

Figure 1. **Left**: map of Nevado de Toluca, Mexico, showing the extent of pyroclastic density current deposits (unit $F_1$ of the Upper Toluca Pumice). The black area are massive deposits (>2 m), the thick dotted line delimits stratified deposits (>2 m) and the dashed line shows the

maximum extent of $F_1$. Thick line shows the road to the town of Tenango (star). Circles indicate thickness measurements, triangles refer to sample locations, and square locates section of Fig. 2. **Right**: stratigraphic profile of $F_1$ showing the main facies and representative grain size distributions [size (in mm) = $2^{-\phi}$]. In valleys, massive facies thickens markedly and the basal contact of stratified facies is often erosional.

Figure 2. Sedimentological data at the downstream transition from massive to stratified deposits (Basal unit). **A)** Sketch of the outcrop with sample location. **B)** Density sorting (as expressed by the difference between pumice and lithics) between the massive facies (ATO130), a poorly sorted planar bed (ATO129), and a coarse planar bed (ATO128, see also Fig. 5a). **C)** Difference in grain size distribution.

Figure 3. Characteristic shape (length versus thickness) of planar beds and dunes. Straight lines are power-law correlations. Coarse beds are gravels and fine beds are sand or finer. Gray area covers the extent of dunes from other deposits (Taal, Laacher, El Chichon, Ubehebe, and Bandelier; Sigurdsson et al., 1987).

Figure 4. Sedimentological data of the stratified facies at Toluca. Dotted lines are samples with a dominant pumice-rich coarse mode (labels are sample numbers, see also Fig. 5a). **A)** Grain size distribution of 11 bulk samples (gray area). Solid line is a representative sample showing the polymodal nature of bulk stratified layers. **B)** Grain size distribution of 9 beds. Solid line is a representative sample showing the unimodal nature of individual beds. **C)** Density sorting of 20 samples (gray area).

Figure 5. **A)** Size distributions of pumice (thick lines) and lithics (thin lines) of 4 individual stratified beds and 1 fall deposit ($PC_2$, Arce et al., 2003) at Toluca. Pumice and lithic modes are indicated when present (thick and thin vertical lines, respectively). **B)** Hydraulic

equivalences for fallout, saltation, and rolling (inset is conceptual sketch). For each mechanism, lines relate lithic (2500 kg $m^{-3}$) size to pumice [702 ± 114 kg $m^{-3}$ (1$\sigma$) Arce, 2003] size. Short-dotted line applies to falling/saltating clasts (Equ. 1) and packed rolling (Equ. 8); solid line applies to shear-induced rolling (Equ. 8); long-dotted line applies to collision-induced rolling (Equ. 10). Gray areas are ranges of equivalences caused by the spread in UTP densities. Symbols indicate observed ratios for samples in A): samples deposited by rolling (triangles), by fallout (open star), and by fallout/saltation followed by rolling (squares). Errors not shown are smaller than symbols.

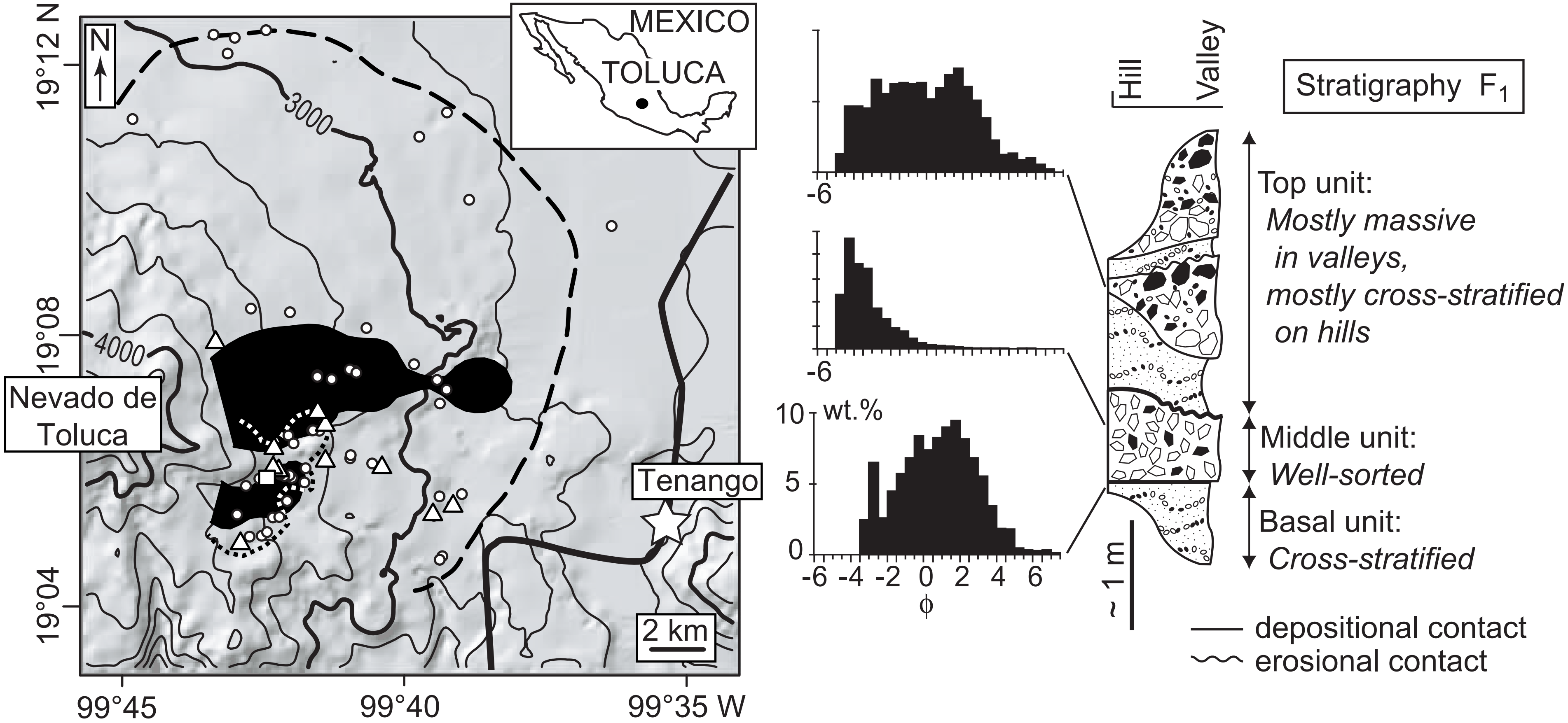
MEXICO
TOLUCA
N
3000
4000
Nevado de Toluca
Tenango
2 km
19°12 N
19°08
19°04
99°45
99°40
99°35 W
-6
-6
10 wt.%
5
0
-6 -4 -2 0 2 4 6
ϕ
Hill
Valley
Stratigraphy $F_1$
Top unit:
Mostly massive in valleys, mostly cross-stratified on hills
Middle unit:
Well-sorted
Basal unit:
Cross-stratified
~ 1 m
depositional contact
erosional contact

**FIGURE 1**

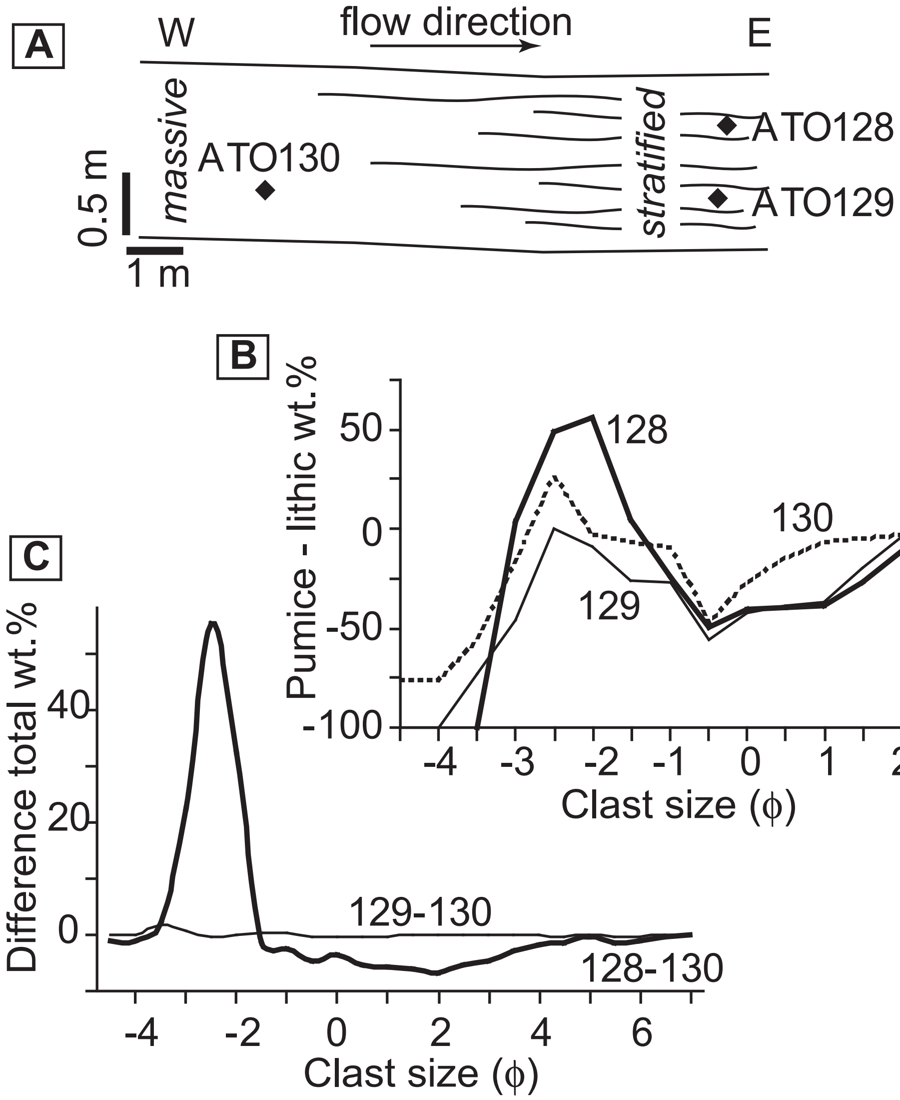
A
W
flow direction
E
massive
ATO130
stratified
ATO128
ATO129
0.5 m
1 m
B
Pumice - lithic wt.%
50
0
-50
-100
128
130
129
-4
-3
-2
-1
0
1
2
Clast size (ϕ)
C
Difference total wt.%
40
20
0
129-130
128-130
-4
-2
0
2
4
6
Clast size (ϕ)

**FIGURE 2**

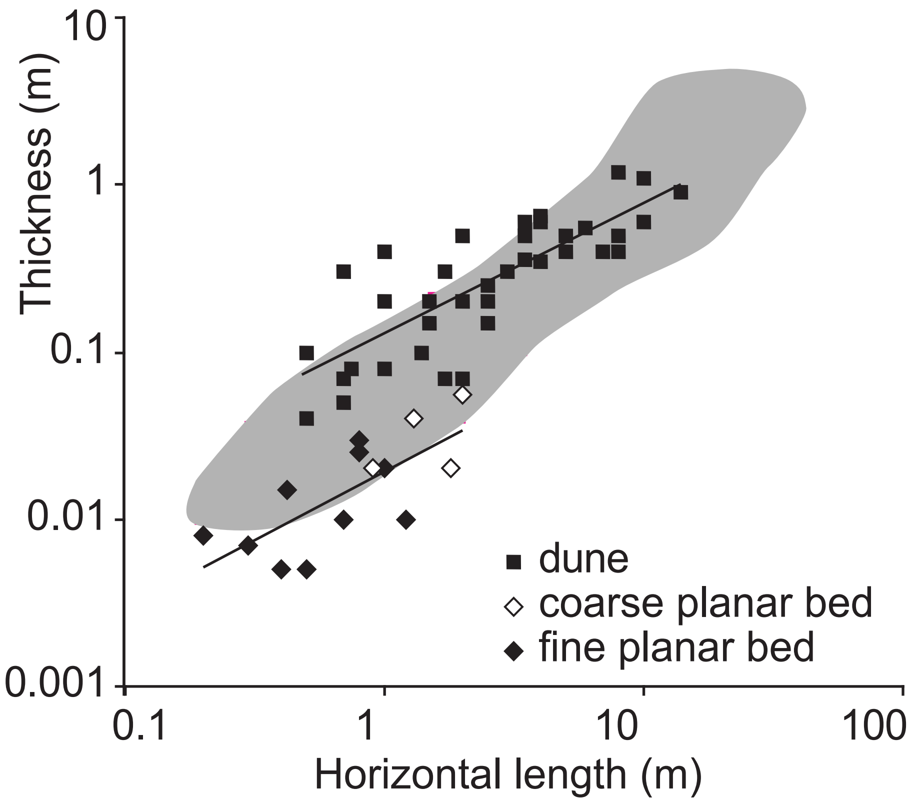
10
1
0.1
0.01
0.001
Thickness (m)
0.1
1
10
100
Horizontal length (m)
dune
coarse planar bed
fine planar bed

**FIGURE 3**

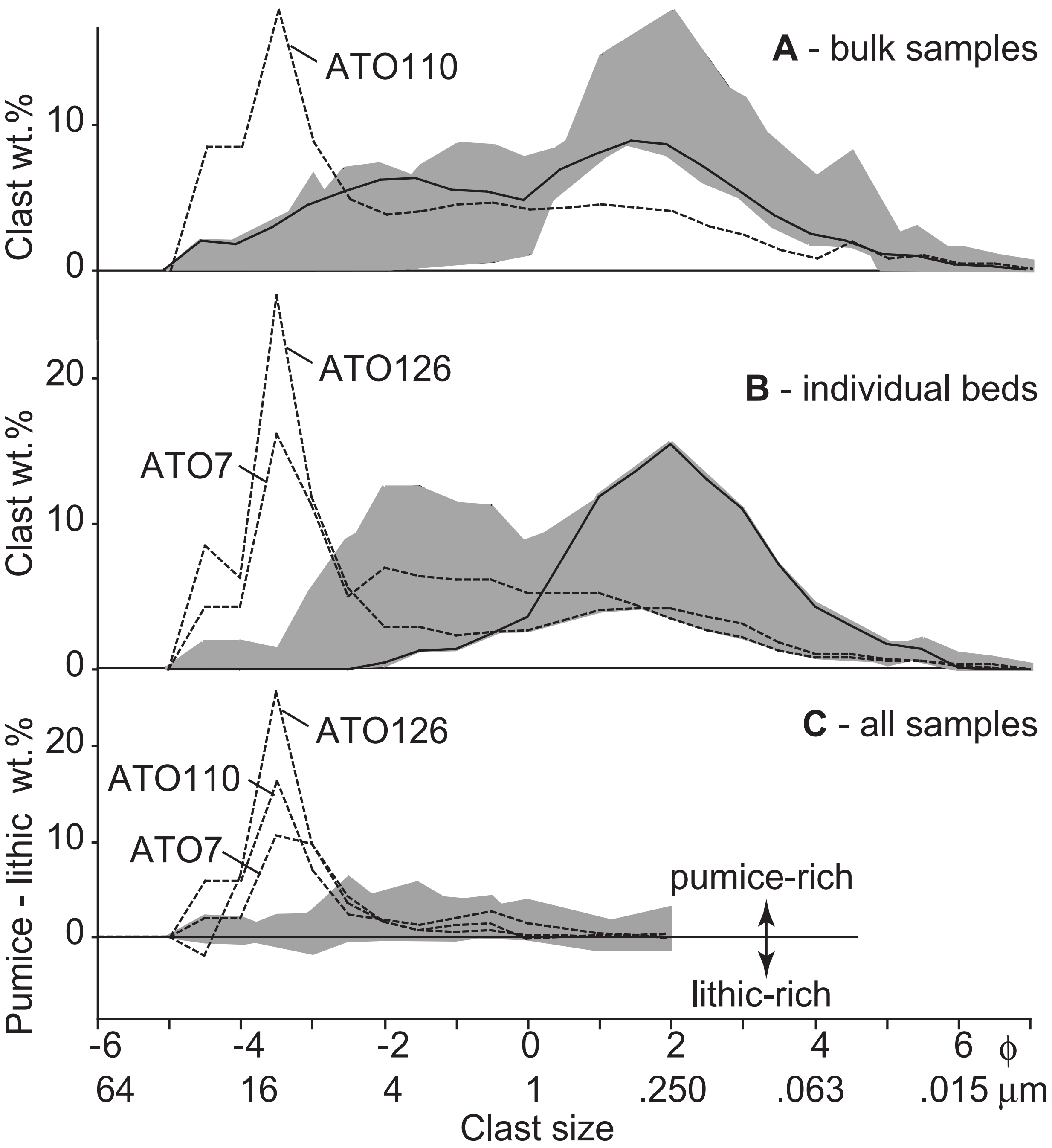

A - bulk samples
ATO110
Clast wt.%
10
0
B - individual beds
ATO126
ATO7
Clast wt.%
20
10
0
C - all samples
ATO126
ATO110
ATO7
Pumice - lithic wt.%
20
10
0
pumice-rich
lithic-rich
-6
-4
-2
0
2
4
6
ϕ
64
16
4
1
.250
.063
.015 μm
Clast size


**FIGURE 4**

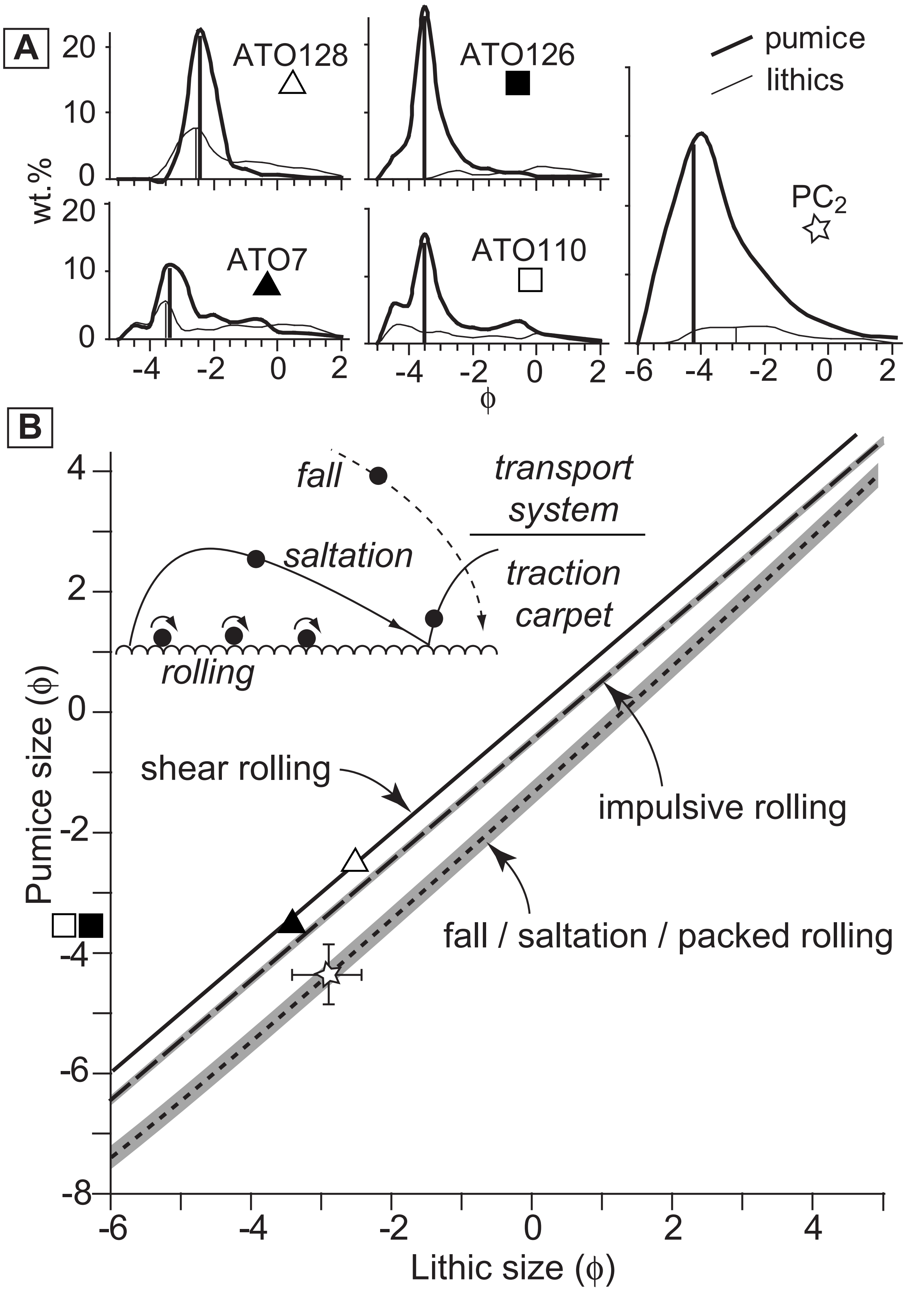

A
20
10
0
wt.%
ATO128
ATO126
pumice
lithics
ATO7
ATO110
PC₂
-4 -2 0 2
-6 -4 -2 0 2
ϕ
B
fall
transport system
saltation
traction carpet
rolling
shear rolling
impulsive rolling
fall / saltation / packed rolling
Pumice size (ϕ)
Lithic size (ϕ)
4
2
0
-2
-4
-6
-8


**FIGURE 5**